

## Global patterns and determinants of forest canopy height

SHENGLI TAO,<sup>1</sup> QINGHUA GUO,<sup>2</sup> CHAO LI,<sup>1</sup> ZHIHENG WANG,<sup>1</sup> AND JINGYUN FANG<sup>1,3</sup>

<sup>1</sup>*Department of Ecology, College of Urban and Environmental Sciences, and Key Laboratory for Earth Surface Processes of the Ministry of Education, Peking University, Beijing 100871 China*

<sup>2</sup>*State Key Laboratory of Vegetation and Environmental Change, Institute of Botany, Chinese Academy of Sciences, Beijing 100093 China*

**Abstract.** Forest canopy height is an important indicator of forest biomass, species diversity, and other ecosystem functions; however, the climatic determinants that underlie its global patterns have not been fully explored. Using satellite LiDAR-derived forest canopy heights and field measurements of the world's giant trees, combined with climate indices, we evaluated the global patterns and determinants of forest canopy height. **The mean canopy height was highest in tropical regions, but tall forests (>50 m) occur at various latitudes.** Water availability, quantified by the difference between annual precipitation and annual potential evapotranspiration (P–PET), was the best predictor of global forest canopy height, which supports the hydraulic limitation hypothesis. However, in striking contrast with previous studies, the canopy height exhibited a hump-shaped curve along a gradient of P–PET: it initially increased, then peaked at approximately 680 mm of P–PET, and finally declined, which suggests that excessive water supply negatively affects the canopy height. This trend held true across continents and forest types, and it was also validated using forest inventory data from China and the United States. Our findings provide new insights into the climatic controls of the world's giant trees and have important implications for forest management and improvement of forest growth models.

**Key words:** climatic indices; forest canopy height; geoscience laser altimeter system; giant trees; light detection and ranging; potential evapotranspiration; RH100; tallest tree; water supply.

### INTRODUCTION

Forest canopy height is among the most important indicators of forest biomass, site quality, species diversity, and several other ecosystem functions (MacArthur and MacArthur 1961, Fang et al. 2006, Moles et al. 2009). Quantifying the patterns and determinants of forest canopy height at the global scale is therefore important for ecological studies, especially given the onset of climate change. According to previous research, forest canopy height can be influenced by various factors, among which water supply might be the most critical (this is referred to as “the hydraulic limitation hypothesis”; Ryan and Yoder 1997, Koch et al. 2004, Moles et al. 2009). Nonetheless, a quantitative description of the determinants underlying its global patterns has rarely been documented, mainly because of the lack of global forest height data.

Satellite Light Detection and Ranging (LiDAR) is a state-of-the-art remote sensing technique that provides

worldwide measurements of forest canopy height (Harding and Carabajal 2005). Satellite LiDAR data have recently been used to quantify the global distributions (Simard et al. 2011, Wang et al. 2016) and determinants (Klein et al. 2015, Zhang et al. 2016) of forest canopy height. However, modeled satellite LiDAR data, instead of original data, are often utilized. For example, Klein et al. (2015) explored the relationship between satellite LiDAR-derived global forest canopy heights and a climatic moisture index calculated as the difference between annual precipitation and annual potential evapotranspiration (hereafter referred to as P–PET; Rind et al. 1990). The results of Klein et al. (2015) suggested that P–PET could predict forest canopy height at the global scale and that canopy heights peaked at 45 m beyond a P–PET threshold of 500 mm. However, the forest canopy heights used by Klein et al. (2015) were not direct LiDAR canopy heights but rather modeled values that were produced by combining satellite LiDAR data and ancillary climatic variables, including precipitation and temperature (Simard et al. 2011). The modeling procedure might have led to an underestimation of canopy

Manuscript received 5 April 2016; revised 11 August 2016; accepted 8 September 2016. Corresponding Editor: J. Nicholas.

<sup>3</sup>E-mail: jyfang@urban.pku.edu.cn

heights (Simard et al. 2011). Moreover, P–PET can be autocorrelated with the precipitation and temperature data that are enclosed in the modeled canopy height product (Klein et al. 2015).

The purpose of this study is to re-evaluate the global patterns and, especially, the determinants of forest canopy height based on original satellite LiDAR-observed canopy heights and various climatic indices. Moreover, we intend to validate the remote-sensing-based results using massive ground survey plots.

## MATERIALS AND METHODS

### *Global forest canopy heights derived from satellite LiDAR*

The Geoscience Laser Altimeter System (GLAS) sensor on board the Ice, Cloud, and Land Elevation Satellite (ICESat) was launched on January 12, 2003. The GLAS sensor emits laser beams to the Earth's surface to characterize three-dimensional global surface structures, and it generates 65-m diameter laser spots that are spaced 172 m apart along ICESat's ground track (Harding and Carabajal 2005). GLAS data are waveforms that can be used to calculate the canopy top height (or maximum canopy height) of a forest (referred to as RH100 in LiDAR terminology, Harding and Carabajal 2005). To calculate the RH100 values for the global forest, we downloaded GLAS14 (version 34) and GLAS01 data covering the temporal period from May 20 to June 23, 2005, from the National Snow and Ice Data Center website (<http://nsidc.org/data/icesat>). GLAS laser spots within forest regions were identified according to the global land cover dataset GlobCover 2009, which has a spatial resolution of 0.00277° (~300 m; [http://due.esrin.esa.int/page\\_globcover.php](http://due.esrin.esa.int/page_globcover.php); version 2.3, last accessed November 12, 2015). Then, RH100 was calculated as the height difference between the signal start and the ground peak, with the ground peak determined as the last Gaussian peak (Simard et al. 2011). RH100 values can be distorted by cloud contamination, atmospheric saturation, and terrain slope; thus, we screened low-quality GLAS data using stringent criteria (Lefsky et al. 2007, Simard et al. 2011, see Appendix S1: Table S1 for the filtering procedures). After filtering, the remaining 108,768 GLAS shots covered all of the world's forest types (Appendix S1: Table S2), and they were used in our analysis.

### *Field-measured giant trees*

The GLAS sensor covers large areas of forests and may miss some of the world's tallest trees due to its spatial separation of individual spots. Therefore, we compiled a database of the world's giant trees, including the tallest tree on Earth (Koch et al. 2004, also see Appendix S2 for the entire list of giant trees), by reviewing publications and credible websites in which giant trees across the world are reported. We then incorporated these data into our data analysis.

### *Climate data*

Based on previous studies (Rind et al. 1990, Moles et al. 2009, Klein et al. 2015, Zhu et al. 2015), climatic indices were selected as potential determinants of global forest heights; the climatic indices include four temperature indices (annual mean temperature [AMT], mean temperature of the wettest quarter [MTWQ], mean temperature of the driest quarter [MTDQ], and mean temperature of the coldest quarter [MTCQ]) and four moisture indices (annual precipitation [AP], precipitation of the wettest month [PWM], the difference between annual precipitation and annual potential evapotranspiration [P–PET], and the difference between annual precipitation and annual actual evapotranspiration [P–AET]). Other climatic indices were not used because of their high correlations with the chosen ones.

All the climate data were obtained from WorldClim at a spatial scale of 0.00833° (~1 km) for the period 1950–2000 (Hijmans et al. 2005), except for the PET and AET data. For a rigid and comprehensive evaluation of the relationships between water availability and global forest canopy heights, we used two datasets for both PET and AET. The two PET datasets, each of which has a spatial resolution of 0.00833° (~1 km), were calculated using the Thornthwaite formula (Thornthwaite PET hereafter; Fang and Yoda 1990) or the Hargreaves formula (Hargreaves PET hereafter; <http://www.cgiar-csi.org/data>; last accessed November 12, 2015). For the two AET datasets, one has a spatial resolution of 0.00833° (~1 km) and was calculated using monthly climate data from WorldClim and the Thornthwaite formula, whereas the other has a spatial resolution of 5 arc-minutes (~10 km) for the period 1961–1990 and was provided by the United Nations Food and Agriculture Organization (FAO; <http://www.fao.org/geonetwork/srv/en/main.home>).

### *Forest inventory data*

We used the National Forest Resource Inventory Database of the State Forestry Administration, China (FRID; State Forestry Administration of China, 2009) and the Forest Inventory Analysis (FIA) database for the United States (<http://apps.fs.fed.us/fiadb-downloads/datamart.html>; last accessed November 15, 2015) to validate the results calculated using the GLAS data and field-measured giant trees. The national forest inventory of China collectively includes >90,000 plots that range from boreal to tropical forests (Guo et al. 2013). The FIA program includes >960,000 plots that span from Alaska in the north to Puerto Rico in the south.

### *Statistical analysis*

Similar to Klein et al. (2015), the maximum observed forest canopy heights in each 0.1° increment in temperature and 1-mm and 10-mm increments in moisture were extracted and fitted against the corresponding climate indices. We

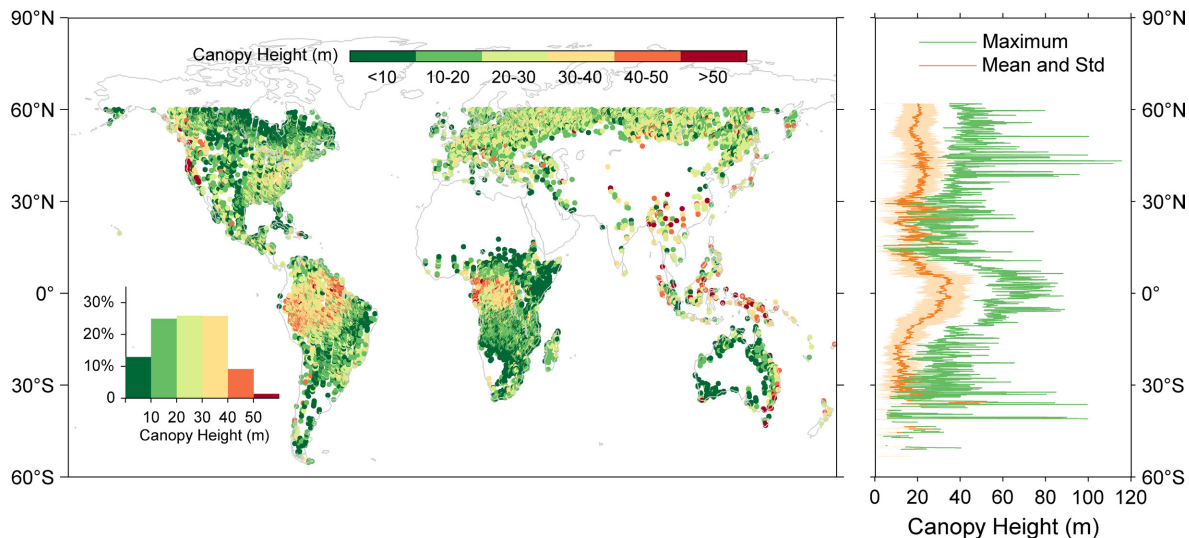


FIG. 1. Spatial distribution of forest canopy heights derived from the GLAS data and field-measured giant trees and their latitudinal patterns. The inset graph shows the frequency distribution of the forest canopy heights.

tested various regression methods, including one polynomial regression (i.e., quadratic regression), and three peak regressions (i.e., log-normal, Weibull, and Gaussian regressions). Because log-normal regression performed consistently better than Weibull and Gaussian regressions as judged by the  $R^2$  values, we reported only the results of the log-normal regression for the category of peak regression. All curve-fitting procedures were performed using the MATLAB 2013 software package (MathWorks 2013).

## RESULTS

### *Biogeographic patterns of forest canopy height*

As shown in the spatial and latitudinal patterns of global forest canopy heights (Fig. 1), the mean heights were highest in tropical forests, which confirms the result of Moles et al. (2009) and Simard et al. (2011). Although the maximum height of the forests in some degree exhibited a similar latitudinal trend to that of the mean height, it had three peaks that occurred in tropical forests and in forests at the mid-latitudes (approximately 40°N and 40°S), where the tallest known trees on Earth were recorded (Koch et al. 2004, Sillett et al. 2015). Tall forests (>50 m) were widely distributed in different latitudes, although they accounted for only 1.3% of the total forest area (inset graph in Fig. 1).

### *Relationships between climatic indices and canopy heights*

Forest canopy heights were poorly fitted by temperature indices using either of the fitting techniques, with  $R^2$  that ranged from 0.21 to 0.30 (Appendix S3: Figs. S1 and S2). In general, canopy heights increased with increasing

temperature but dropped sharply beyond approximately 25°C of AMT (Appendix S3: Fig. S1a–d). This reduction might be caused by a varying water supply rather than changing temperature because the temperature in these forested areas varied only within 4°C, whereas the water availability, which was quantified with P–PET, as shown in the following sections, differed by as much as 3,000 mm (Appendix S3: Fig. S3). Forests were tall in very cold regions, with MTCQs that ranged from –30 to –10°C (Appendix S3: Fig. S1d). All of these facts suggest that temperature might not be the primary determinant of global forest canopy heights.

Compared with temperature indices, the moisture indices predicted well the global forest canopy heights with  $R^2$  up to 0.72 (Appendix S3: Figs. S1 and S2), which suggest a dominant role of water supply in determining forest canopy heights globally. Our data further demonstrate that the relationship between moisture and canopy heights differed strikingly from recent studies, which reported that canopy heights either increased continuously with increasing moisture (Givnish et al. 2014) or peaked at high moisture levels (Klein et al. 2015). As shown in Fig. 2 (also see Appendix S3: Fig. S2e–i), the canopy height exhibited a hump-shaped trend with increasing moisture levels (P–PET): it initially increased, then peaked at approximately 680 mm of P–PET, and finally declined, regardless of the moisture index used. This result suggests that an excessive water supply has negative effects on forest canopy height.

Among all the moisture indices used, P–PET had the best fit when evaluated with either of the curve-fitting methods (Appendix S3: Figs. S1i and S2i). Furthermore, the relationship between P–PET and canopy height conformed most closely to a log-normal distribution, with the fitted  $R^2$  values of 0.72 and 0.79 for 1 mm and 10 mm

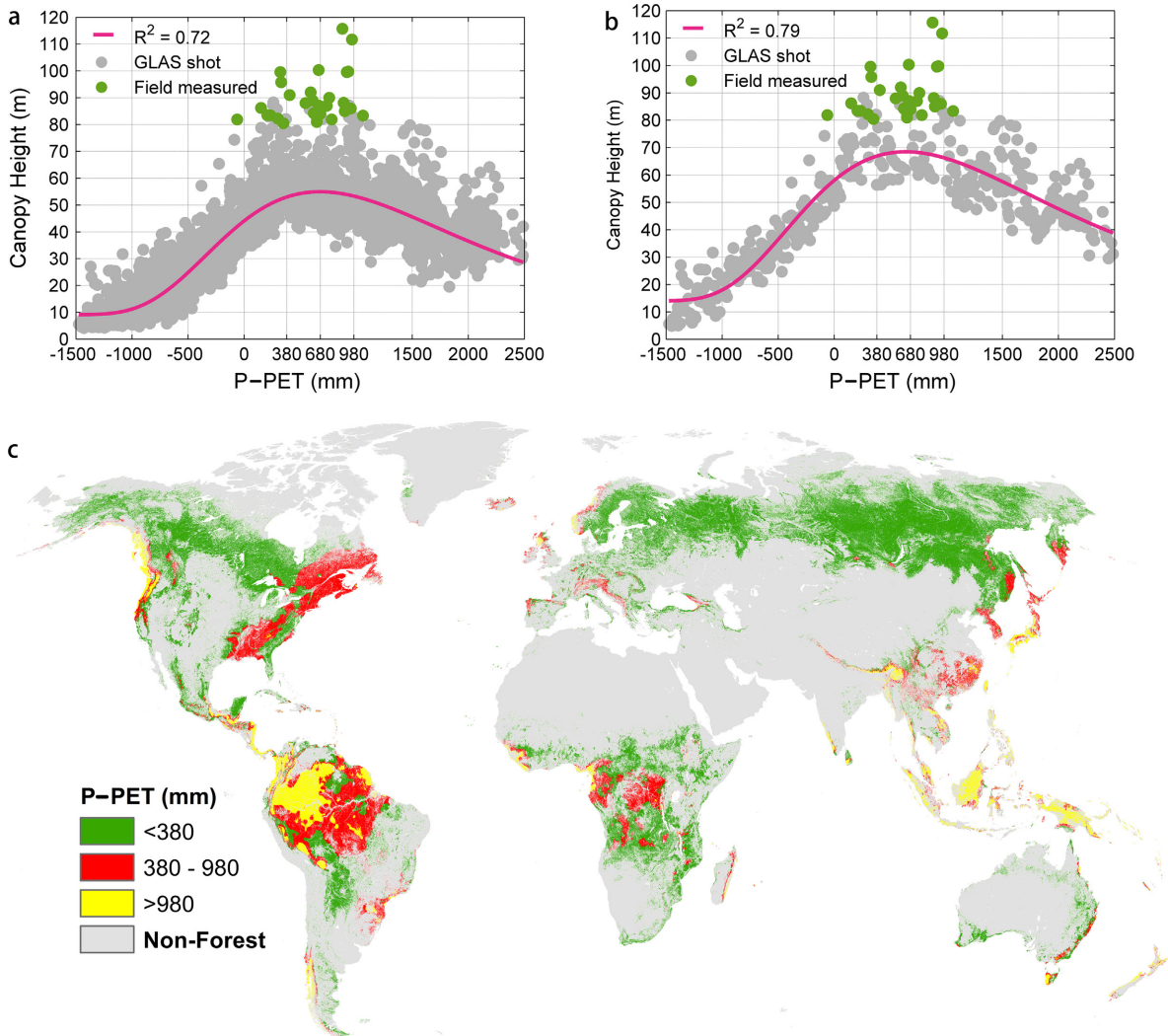


FIG. 2. Relationships between P–PET and global maximum forest canopy heights in every (a) 1-mm increment and (b) 10-mm increment in P–PET; (c) the distribution of P–PET values in geographic space. PET was calculated using the Thornthwaite equation. Red lines are the fitted log-normal models. The overall trend remains when Hargreaves PET is used (Appendix S3: Fig. S6).

increments in P–PET, respectively (Fig. 2a, b; Appendix S3: Table S1). Thus, using P–PET as the predictor of forest canopy heights, combined with log-normal regressions, we determined the relationship of forest canopy heights with water availability in geographic space (Fig. 2c). As predicted by P–PET and log-normal regression, the world's tallest forests can be found in certain geographical regions with approximately  $680 \pm 300$  mm of P–PET. These regions included the east and west coasts of North America, Tasmania and Victoria of Australia, Europe, the eastern Himalayas, Russian Far East, and Southeast Asian, Amazonian, and African tropical forests (Fig. 2c). Notably, 48 out of 55 (87%) field-measured giant trees were located within these regions (Appendix S2), including the tallest trees on Earth, which suggests that the world's giant trees might

grow in climates of similar moisture level. Forests whose canopy heights declined because of high P–PET values were mainly located in the tropical Amazon and other areas such as Asia, New Zealand, and the west coast of the USA. The overall trend of a decrease in canopy height at high P–PET values holds for different continents, forest types (Appendix S3: Figs. S4 and S5), and different PET products (Appendix S3: Fig. S6).

#### DISCUSSION

This study evaluated the global patterns and determinants of forest canopy height. The global pattern of forest canopy height found in this research generally confirms the results of Simard et al. (2011), with the highest mean forest canopy height occurring in tropical regions

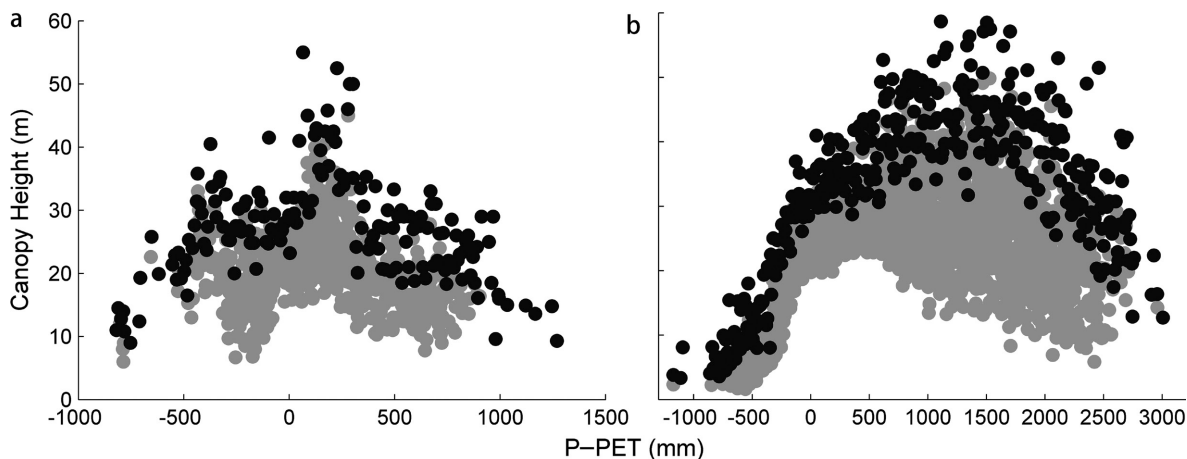


FIG. 3. Relationships between P-PET and forest inventory heights from (a) China and (b) the United States. Grey and black dots were the maximum canopy heights in each 1-mm and 10-mm increment in P-PET, respectively. Declining trends in forest canopy heights at high P-PET values were observed, thereby confirming the results obtained using the GLAS data.

and tall forests (>50 m) appearing in a wide latitudinal range. Furthermore, our results highlight the dominant role of water availability in controlling forest canopy height globally (Fig. 2), which supports the hydraulic limitation hypothesis (Ryan and Yoder 1997). In previous studies, Givnish et al. (2014) found that canopy heights continuously increased with increasing moisture in Victoria, Australia, and Klein et al. (2015) reported that canopy heights peaked beyond a moisture threshold at global scale. However, in striking contrast with these studies, we found that high P-PET (>680 mm) had negative effects on forest height, thereby resulting in lower canopy heights (Fig. 2, Appendix S3: Figs. S1–S6). The result of Givnish et al. (2014) was based on limited data of *Eucalyptus regnans* in nineteen sites with low and intermediate moisture conditions but possibly omitted trees growing in higher moisture levels (Appendix S3: Fig. S4e). Although both Klein et al. (2015) and our study are based on satellite LiDAR-derived canopy heights, they used the modeled RH100 values, whereas we used the original RH100, which are not auto-correlated with P-PET and do not suffer from underestimation of forest heights (Simard et al. 2011). RH100 can be distorted in sloping terrain; therefore, we screened low-quality GLAS data strictly according to previous studies (Harding and Carabajal 2005, Lefsky et al. 2007, Simard et al. 2011). We acknowledge that there might still be uncertainties in the RH100 values after filtering, but the new relationship between water input and forest canopy heights is robust because it holds for different moisture indices, continents, forest types and PET products (Appendix S3: Figs. S1–S2, and S4–S6). Our findings can also be evidenced by existing plot studies. For example, Megonigal et al. (1997) found significantly lower net primary production (NPP) in wet sites than in dry sites in southeastern floodplain forests in USA. Schuur (2003) reported a negative relationship between mean annual precipitation and NPP in perhumid ecosystems. Marks et al. (2016) found

relatively lower maximum tree height in southern Florida, which can be partly attributed to the increases in the soil water-logging tolerance of trees. More importantly, using forest inventory data from China and USA, we found that forest canopy heights decreased with very high water availability (Fig. 3), which strongly supports the results derived from the GLAS data in this study.

Why does forest canopy height decrease with increasing water availability? Phyto-physiologically, water in excess of biological demand leads to nutrient leaching in soil (Kozłowski 1984, Schuur and Matson 2001, Lambers et al. 2008), reduction of the soil O<sub>2</sub> supply, and formation of aerenchyma in roots, which inhibit root growth and reduce the supporting power of roots (Blom and Voesenek 1996, Lambers et al. 2008). Extra water supply also affects photosynthesis directly by inducing stomatal closure (Blanke and Cooke 2004) and reducing radiation inputs (Schuur 2003). These physiological processes might be associated with the decline in forest canopy height at high moisture levels. In addition, the cloud cover in these extremely wet areas can be high, which can possibly lead to light limitation of forest growth (Graham et al. 2003).

The relationship between P-PET and canopy height has several important implications. First, it might provide new insights into the climatic determinant of world's giant trees (Fig. 2). Second, the fitted models between P-PET and canopy heights can be used to estimate the height potential and, consequently, carbon sequestration potential of world's forests (Silleet et al. 2015, Chazdon et al. 2016), given the surprisingly linear relationship between carbon density and forest height at closed forests across a large-scale (Fang et al. 2006). Third, the P-PET vs. canopy height relationship can also be used for forest management practices by identifying suitable regions for forestation and to investigate the responses of forests to projected changes in precipitation (Intergovernmental Panel on Climate Change [IPCC] 2007). Moreover, the finding that forest canopy height decreases at high levels

of water availability might also be useful for modification of forest growth models and global carbon cycle models (Schoor 2003).

#### ACKNOWLEDGMENTS

We thank two anonymous reviewers and editor Nathan Kraft for their constructive comments on the earlier draft. This work was partly funded by National Natural Science Foundation of China (#31321061 and 31330012), and National Basic Research Program of China on Global Change (2010CB950600).

#### LITERATURE CITED

- Blanke, M. M., and D. T. Cooke. 2004. Effects of flooding and drought on stomatal activity, transpiration, photosynthesis, water potential and water channel activity in strawberry stolons and leaves. *Plant Growth Regulation* 42:153–160.
- Blom, C. W. P. M., and L. A. C. J. Voesenek. 1996. Flooding: the survival strategies of plants. *Trends in Ecology & Evolution* 11:290–295.
- Chazdon, R. L., et al. 2016. Carbon sequestration potential of second-growth forest regeneration in the Latin American tropics. *Science Advances* 2:e1501639.
- Fang, J. Y., and K. Yoda. 1990. Climate and Vegetation in China III water balance and distribution of vegetation. *Ecological Research* 5:9–23.
- Fang, J. Y., S. Brown, Y. H. Tang, G. J. Nabuurs, X. P. Wang, and H. H. Shen. 2006. Overestimated biomass carbon pools of the northern mid- and high latitude forests. *Climatic Change* 74:355–368.
- Givnish, T. J., S. C. Wong, H. Stuart-Williams, M. Holloway-Phillips, and G. D. Farquhar. 2014. Determinants of maximum tree height in Eucalyptus species along a rainfall gradient in Victoria, Australia. *Ecology* 95:2991–3007.
- Graham, E. A., S. S. Mulkey, K. Kitajima, N. G. Phillips, and S. J. Wright. 2003. Cloud cover limits net CO<sub>2</sub> uptake and growth of a rainforest tree during tropical rainy seasons. *Proceedings of the National Academy of Sciences of the United States of America* 100:572–576.
- Guo, Z. D., H. F. Hu, P. Li, N. Y. Li, and J. Y. Fang. 2013. Spatio-temporal changes in biomass carbon sinks in China's forests from 1977 to 2008. *Science China Life Sciences* 56:661–671.
- Harding, D. J., and C. C. Carabajal. 2005. ICESat waveform measurements of within-footprint topographic relief and vegetation vertical structure. *Geophysical Research Letters* 32: doi:10.1029/2005GL023471.
- Hijmans, R. J., S. E. Cameron, J. L. Parra, P. G. Jones, and A. Jarvis. 2005. Very high resolution interpolated climate surfaces for global land areas. *International Journal of Climatology* 25:1965–1978.
- IPCC (Intergovernmental Panel on Climate Change). 2007. *Climate change 2007: the physical science basis. Contribution of Working Group I to the Fourth Assessment Report of the Intergovernmental Panel on Climate Change.* Cambridge University Press, Cambridge, UK.
- Klein, T., C. Randin, and C. Körner. 2015. Water availability predicts forest canopy height at the global scale. *Ecology Letters* 18:1311–1320.
- Koch, G. W., S. C. Sillett, G. M. Jennings, and S. D. Davis. 2004. The limits to tree height. *Nature* 428:851–854.
- Kozłowski, T. T. 1984. Plant-responses to flooding of soil. *BioScience* 34:162–167.
- Lambers, H., F. S. Chapin III, and T. L. Pons. 2008. *Plant physiological ecology.* Second edition. Springer-Verlag, New York, New York, USA. Page 355–358.
- Lefsky, M. A., M. Keller, Y. Pang, P. B. de Camargo, and M. O. Hunter. 2007. Revised method for forest canopy height estimation from Geoscience Laser Altimeter System waveforms. *Journal of Applied Remote Sensing* 1: 013537.
- MacArthur, R., and J. W. MacArthur. 1961. On bird species-diversity. *Ecology* 42:594–598.
- Marks, C. O., H. C. Muller-Landau, and D. Tilman. 2016. Tree diversity, tree height and environmental harshness in eastern and western North America. *Ecology Letters* 19:743–751.
- MathWorks. 2013. MATLAB. The MathWorks, Inc., Natick, Massachusetts, USA.
- Megonigal, J. P., W. H. Conner, S. Kroeger, and R. R. Sharitz. 1997. Aboveground production in Southeastern floodplain forests: a test of the subsidy-stress hypothesis. *Ecology* 78:370–384.
- Moles, A. T., D. I. Warton, L. Warman, N. G. Swenson, S. W. Laffan, A. E. Zanne, A. Pitman, F. A. Hemmings, and M. R. Leishman. 2009. Global patterns in plant height. *Journal of Ecology* 97:923–932.
- Rind, D., R. Goldberg, J. Hansen, C. Rosenzweig, and R. Ruedy. 1990. Potential evapotranspiration and the likelihood of future drought. *Journal of Geophysical Research-Atmospheres* 95:9983–10004.
- Ryan, M. G., and B. J. Yoder. 1997. Hydraulic limits to tree height and tree growth. *BioScience* 47:235–242.
- Schoor, E. A. G. 2003. Productivity and global climate revisited: the sensitivity of tropical forest growth to precipitation. *Ecology* 84:1165–1170.
- Schoor, E. A. G., and P. A. Matson. 2001. Net primary productivity and nutrient cycling across a mesic to wet precipitation gradient in Hawaiian montane forest. *Oecologia* 128:431–442.
- Sillett, S. C., R. Van Pelt, R. D. Kramer, A. L. Carroll, and G. W. Koch. 2015. Biomass and growth potential of *Eucalyptus regnans* up to 100 m tall. *Forest Ecology and Management* 348:78–91.
- Simard, M., N. Pinto, J. B. Fisher, and A. Baccini. 2011. Mapping forest canopy height globally with spaceborne lidar. *Journal of Geophysical Research-Biogeosciences* 116: doi: 10.1029/2011JG001708.
- State Forestry Administration of China. 2009. Seventh national forest resource inventory report (2004–2008). State Forestry Administration of the People's Republic of China, Beijing, China.
- Wang, Y. Y., G. C. Li, J. H. Ding, Z. D. Guo, S. H. Tang, C. Wang, Q. N. Huang, R. G. Liu, and J. M. Chen. 2016. A combined GLAS and MODIS estimation of the global distribution of mean forest canopy height. *Remote Sensing of Environment* 174:24–43.
- Zhang, J., S. E. Nielsen, L. F. Mao, S. B. Chen, and J. C. Svenning. 2016. Regional and historical factors supplement current climate in shaping global forest canopy height. *Journal of Ecology* 104:469–478.
- Zhu, J. L., Y. Shi, L. Q. Fang, X. E. Liu, and C. J. Ji. 2015. Patterns and determinants of wood physical and mechanical properties across major tree species in China. *Science China Life Sciences* 58:602–612.

#### SUPPORTING INFORMATION

Additional supporting information may be found in the online version of this article at <http://onlinelibrary.wiley.com/doi/10.1002/ecy.1580/supinfo>